ACS APPLIED MATERIALS & INTERFACES

Research Article

www.acsami.org

Annealing of P3HT:PCBM Blend Film—The Effect on Its Optical Properties

Annie Ng,[†] Xiang Liu,[†] Chap Hang To,[‡] Aleksandra B. Djurišić,*[,†] Juan Antonio Zapien,*[,‡] and Wai Kin Chan[§]

[†]Department of Physics, The University of Hong Kong, Pokfulam Road, Hong Kong

[‡]Center of Super Diamond and Advanced Films (COSDAF) and Department of Physics and Materials Science, City University of Hong Kong, Tat Chee Avenue, Kowloon Tong, Hong Kong

[§]Department of Chemistry, The University of Hong Kong, Pokfulam Road, Hong Kong

Supporting Information

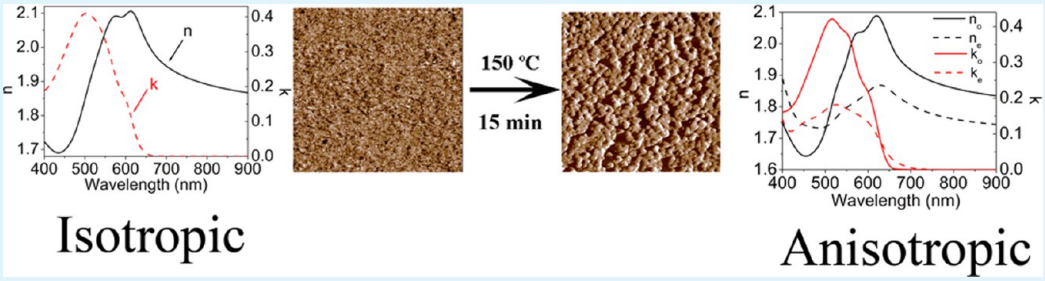

ABSTRACT: Annealing is a common method to improve the efficiency of polymer photovoltaic cells. Annealing changes the microphase separation in a polymer blend film and typically also results in a change in its optical properties. We investigated the optical properties of poly(3-hexylthiophene) (P3HT):[6,6]-phenyl C_{61} butyric acid methyl ester (PCBM) before and after thermal annealing using spectroscopic ellipsometry and transmission measurements, with simultaneous fitting of samples with different thicknesses to ensure reliability of extracted index of refraction values. We found that, after annealing, it is necessary to consider an anisotropic model to describe the properties of P3HT:PCBM blend films, which reflects the increased order of P3HT chains as a result of annealing. Different fitting models (simple anisotropic layer, graded isotropic, graded anisotropic model, generalized oscillator, and oscillator model including Huang–Rhys vibronic envelope) have been compared and discussed. The effect of the number of samples used for fitting and surface roughness corrections is also discussed.

KEYWORDS: *polymer films, spectroscopic ellipsometry, solar cells*

1. INTRODUCTION

Polymer solar cells have been attracting increasing attention recently because of their outstanding properties, such as low cost and possible use of flexible substrates, with associated advantages of light weight, high mechanical flexibility, and possibility of roll-to-roll processing. A number of different polymer materials have been used in organic photovoltaic (OPV) cells. Poly(3-hexylthiophene) (P3HT):[6,6]-phenyl C_{61} butyric acid methyl ester (PCBM) remains one of the most common bulk heterojunction material combinations, with over 1000 published articles on this material combination in the period from 2002 to 2010.[1] Reported efficiencies range from below 0.5% to ~5%, with the average value of ~3%.[1] Thus, the solar cells based on P3HT:PCBM have been comprehensively investigated. For example, the influence of different additives,[2] casting solvents,[3] molecular weight,[4] regioregularity,[5] annealing time,[6] and temperature,[6] etc. has been studied. It is well recognized that the morphology of the P3HT:PCBM plays a significant role in the device performance.[7] Morphology of the films can be controlled in different ways (heating, solvent annealing, additives, etc.). The effects of blend layer morphology changes can be clearly observed in the absorption spectra.[2,3,7] Morphologies favorable for good photovoltaic performance typically exhibit more intense absorption with more pronounced peaks.[2,3,7]

To model and understand the factors affecting the performance of solar cells, knowledge of optical properties of the layers in the device is essential. While a large number of research papers in polymer photovoltaics concentrate on the development of novel materials for solar cell applications, optimization of device architecture, in particular, light trapping, is necessary if polymer solar cells aim to become competitive with inorganic solar cells, which commonly include optimized contacts, antireflective coatings, and/or light-trapping structures. Such optimization of device architecture requires accurate

Received: January 31, 2013
Accepted: April 29, 2013
Published: April 29, 2013

   dx.doi.org/10.1021/am4004232 | ACS Appl. Mater. Interfaces 2013, 5, 4247–4259

characterization of the optical properties of all the layers in the device.

The optical properties of a variety of polymer films, including P3HT and P3HT:PCBM blends, have been reported in the literature.[8−23] Unlike absorption measurements, which only provide an estimate of the absorption coefficient,[12,13] spectroscopic ellipsometry (SE) enables determination of both real and imaginary parts of the complex index of refraction $N = n - ik$, which is needed for modeling the light propagation through an OPV cell.[8] Even though numerous spectroscopic ellipsometry studies have been reported for P3HT[10,22] and P3HT:PCBM films,[8,11,14,15] studies that report fitting of multiple samples[8,14,15] have been scarce, as well as studies that report combinations of different techniques (SE + transmittance (T) and/or reflectance (R) measurements).[8,11,22] However, obtaining unique and accurate solutions in terms of optical functions of a thin film from spectroscopic ellipsometry generally requires consideration of multiple samples with different thicknesses and/or combinations of SE + T measurements (applicable to transparent substrates only).[24] In particular, the accurate determination of optical anisotropy using SE typically requires either a special sample configuration or a combination of different experimental techniques,[9] such as transmittance and spectroscopic ellipsometry.[10,22] It should be noted that it is not simply a case of using combinations of measurements and multisample fitting to achieve better accuracy (as in, for example, obtaining one more significant digit), but rather a fundamental difference between obtaining accurate optical function representations as opposed to misleading, inconsistent, or even unphysical, results.[18] Complications leading to the high possibility of spurious solutions arise because (i) the highly nonlinear nature of the ellipsometric equations resulting in the appearance of multiple stable solutions (i.e., those for which the MSE shows a local minimum as the model parameters are varied close to the local-minimum value), (ii) the small optical thickness of the samples under consideration, which may be smaller than the condition for interference (the presence of interference effects over the measuring spectral range may assist in detecting spurious solutions), and (iii) the inherent complexity of the samples under consideration that requires multiparameter models and increased risk of spurious solutions from strong parameter cross-correlations. Without following appropriate fitting procedures, obtaining reasonable data that are useful for device modeling and/or understanding the effect of various processing conditions on the properties of the blend film is highly unlikely. In particular, attempts to determine preferential segregation of blend components solely from SE measurements on one sample are unlikely to be successful due to the existence of multiple stable solutions. To fully utilize the benefits of optical characterization methods, such as SE, for solar cell materials, it is essential to fully understand the limitations of the technique, the importance of adopting appropriate models, and the importance of using mutlisample fitting and the combinations of experimental data to obtain reliable solutions. However, the reports of multisample fitting of combinations of measurements are scarce, due to difficulties in obtaining a good fitting solution.

Consequently, the absolute values of n and k obtained in the estimates of the degree of anisotropy, the influence of annealing, and regioregularity on the optical properties of P3HT:PCBM blend films obtained from SE studies on single thickness samples[11] may be less reliable,[8] although the trends observed could be correct. Similar problems could exist for studies of annealing effects,[18−21] including changes in film composition (grading),[20] the use of different effective medium approximations (EMAs),[20] etc., where only SE data or only one sample thickness is considered. In some published works, a combination of an insufficient number of thickness values and an inappropriate model (Lorentz oscillator model, which typically results in an overestimation of absorption below the band gap due to broad wings of a Lorentzian function) can result in obviously unphysical values, such as an extinction coefficient k that increases above 620 nm, and a refractive index $n < 1$ over a large spectral region ∼(1.5−4.0) eV.[18] Thus, the appropriate choice of the oscillator model describing identified/known transitions is of the utmost importance.

The complexity of the materials at hand is further illustrated by the fact that certain experimental conditions have resulted in PCBM segregation,[15] which was optically modeled assuming pure P3HT to be isotropic and further resulted in the need to consider graded P3HT:PCBM layers with the PCBM segregated layer on the film surface.[15] It is, however, noticed that such models should not be assumed in general without an independent verification of the actual sample structure since contradicting results have been reported and the segregation is dependent on the processing condition and P3HT properties. In principle, including more independently confirmed data about the sample in the optical model results in the retrieval of more reliable information from the model fitting.

In our previous work using nonannealed samples of different thicknesses, a unique isotropic model was found to adequately describe the optical response (multiangle of incidence SE and normal incidence T) of pristine P3HT:PCBM blend films.[8] However, annealed P3HT:PCBM solar cells are widely adopted among many research groups since thermal annealing can significantly enhance the photovoltaic performance by improving the crystallization of P3HT and the charge transport characteristics of the blend.[6] Considering the importance of annealing of P3HT:PCBM blends on solar cell performance, it is, therefore, necessary to accurately model the optical functions of annealed P3HT:PCBM blend films.

Significant modification of the absorption spectra of P3HT:PCBM blends commonly occurs as a consequence of annealing, which can result from changes in phase separation (formation of larger aggregates), increased order (crystallization), and increased roughness. It is, therefore, necessary to examine if models used for nonannealed films are valid for annealed blend films. In particular, any preferential molecular orientation in the annealed films could result in uniaxial anisotropy.[9,10] Such preferential orientation is more likely to be present in pure polymer films compared to polymer blends with PCBM, since the introduction of PCBM can interfere with the self-organization of P3HT.[11]

The degree of anisotropy could also be dependent on the molecular weight, as demonstrated on other polymers.[16] In the published literature, both isotropic[18,21] and anisotropic[11,20] models have been used to describe annealed P3HT:PCBM blend films. In this work, we examine the use of isotropic and anisotropic models with multisample analysis and simultaneous fitting of both transmission and ellipsometry data in order to describe annealed P3HT:PCBM blend films. In addition, different oscillator models are considered. Such a simultaneous fitting approach is likely to result in more accurate values of n and k compared to single-sample or single-technique studies previously reported. More importantly, the samples considered

consist of P3HT:PCBM blend films annealed with aluminum electrodes, resulting in realistic annealing conditions used for high photovoltaic performance (solar cells are usually annealed after electrode deposition to suppress excessive crystallization and aggregation) where the electrode has been peeled off just before optical characterization.[25] In contrast with nonannealed samples, we found that it is necessary to include anisotropic effects into account when modeling the optical functions of annealed P3HT:PCBM blend films. We also demonstrate that a simple anisotropic layer (with surface roughness correction) is sufficient for a good description of the optical properties of annealed P3HT:PCBM blend films. Compared to other more complex models used in the literature, such as graded layers,[15,19,20] a simple anisotropic layer results in a better fit of the data (simultaneous fit of ellipsometry and transmittance for multiple samples with different thicknesses), as well as better stability and the uniqueness of fit parameters. Furthermore, we provide a discussion of potential limitations of each approach and suggest guidelines to obtain good quality fitting results for polymer blend films. The procedures described can be applied to novel material combinations in a straightforward manner.

2. EXPERIMENTAL SECTION

P3HT and PCBM were obtained from Rieke Metals (Rieke Metals Lot # 2010-A6-7; M_w = 21 809 g/mol; PDI = 1.63; RR = 95.1%) and Nano C (BJ110729, purity: 99.5%), respectively. P3HT and PCBM in a ratio of 1:0.8 (27 mg/mL) were dissolved in chlorobenzene by stirring separately for 18 h and then mixed together for 2 h at 40 °C before spin-coating. All substrates were cleaned by sonication in toluene, acetone, ethanol, and deionized water sequentially. The substrates were dried under nitrogen and then exposed to UV-ozone for 300 s.

For solar cell fabrication, the poly(3,4-ethylene-dioxythiophene): poly(styrene sulfonate) solution (Clevios PVP Al4083) was passed through a 0.45 μm filter and spin-coated on cleaned ITO on glass substrates (15−20 ohm per square) at 5000 rpm for 2 min, followed by baking the substrate at 120 °C for 20 min in a vacuum oven. The active layer was also passed through a 0.45 μm filter and then spin-coated on the top of PEDOT:PSS at 1000, 1500, 2000, 2500, or 3000 rpm. Immediately after preparation, the samples were kept in high vacuum for 2 h and then transferred to an argon-filled glovebox overnight before evaporation of 100 nm Al electrodes through a shadow mask with a 1 mm radius circle. The devices were annealed at 150 °C for 15 min before $I-V$ measurement. The $I-V$ characteristics of solar cells were measured with a Keithley 2400 sourcemeter under AM 1.5 simulated sunlight illumination (ABET Technologies SUN 2000) at 100 mW/cm^2 (measured by a Molectron Power Max 500D laser power meter).

Additional samples were prepared for optical measurements. Whereas SE measurements were performed on substrates with a roughened back surface to suppress undesired back reflections, standard double-sided polished glass slides were used for transmittance measurements. In all cases, the substrates were cleaned by sonication in toluene, acetone, ethanol, and deionized water sequentially and dried under a nitrogen gas flow and then exposed to UV-ozone for 300 s. The P3HT:PCBM blend films were then spin-coated on the cleaned substrates at spinning speeds ranging from 1000 to 3000 rpm to obtain different thicknesses. The samples were then stored in an argon-filled glovebox overnight before thermal evaporation of 100 nm of aluminum. The P3HT:PCBM samples with aluminum on the top were annealed at 150 °C for 15 min. SE measurements were performed after removing the Al electrode using a 3M tape to expose P3HT:PCBM annealed under realistic photovoltaic device processing conditions. Control samples without annealing, as well as pure P3HT and pure PCBM samples, were also prepared and characterized.

The SE measurements were performed with a J. A. Woollam M-2000 ellipsometer (rotating compensator ellipsometer) using a focusing probe to narrow the spot size to be smaller than the area under the Al electrode. Data were taken from 400 to 900 nm with the step size of 1.6 nm at incident angles of 55, 60, 65, 70, and 75°. Transmission measurements were also performed in the same ellipsometer under a straight-through configuration. The surface morphology of the samples was characterized by atomic force microscopy (AFM) using an Asylum Research MFP3D in semicontact (tapping) mode. AFM measurements were also performed in the same area used for SE measurements after the removal of the Al electrode. The initial thicknesses of P3HT:PCBM films were obtained by scanning electron microscopy (SEM).

SE data analysis was performed following a systematic approach to avoid nongeneral or unphysical solutions as previously described in detail.[8] Effective medium approximation (EMA) was used to model the surface roughness.[8,26,27] A detailed procedure for isotropic model fitting was previously given.[8] In the present case of annealed samples, no satisfactory fit could be obtained using an isotropic model and an anisotropic model needs to be implemented. For both isotropic and anisotropic models, we have considered a generalized oscillator model (GO model)[8] and a model incorporating a Huang−Rhys vibronic envelope (HR model).[22] The detailed description of the HR model, including the physical meaning of the parameters, is given in ref 22. For the GO model, we have limited the number of oscillators to transitions that can be clearly resolved in the spectra, plus one optional higher-energy oscillator (to compensate for transitions outside of the spectral region used for fitting that are sufficiently close to contribute to the optical functions). We emphasize that transitions that cannot be clearly resolved in the experimental (SE and/or T) data can result in optical models with increased parameter correlations; in extreme cases, it is unlikely that the model can be fitted reliably with a unique set of oscillator parameters. For example, the existence of charge transfer states in polymer blend films, including P3HT:PCBM, has been confirmed by alternative optical techniques that show increased sensitivity to such sub-band-gap features, including photocharge extraction by linear increasing voltage (photo-CELIV),[28] Fourier transform photocurrent spectroscopy (FTPS),[29,30] and photothermal deflection spectroscopy (PDS).[30,31] In our case, however, no clear features can be seen in both SE and T spectra at longer wavelengths. Consequently, CT transitions could not be considered as separate oscillators in our modeling. However, it should be noted that peak functions, even Gaussian ones, have extended tails (though lower than in the case of Lorentzian ones), so that it is unlikely that k would be significantly underestimated even in the absence of separate terms accounting for CT absorption (which is typically described as weak absorption[29]). In fact, overestimation of k at long wavelengths due to oscillator tails in fitting SE data is more common than underestimation.

Despite the above considerations on weak absorption features, we found that, in SE data, analysis of pure PCBM films can resolve a very weak feature observed at ∼1.75 eV in the transmission spectra that corresponds to the $S_0 \rightarrow S_1$ transition of PCBM.[28] Even though this feature is very weak, it is well separated from other oscillators, and consequently, it can be reliably fitted. However, no such feature is present near the ∼1.75 eV spectral region for P3HT:PCBM blends; accordingly, we have not included this transition in our optical model. Similarly, transitions observed at longer wavelengths (lower energies) in various spectroscopies using different perturbations (laser excitation, magnetic, electrical)[32] are not observable in SE and T data.

In addition to the GO model described in detail above, we also consider the HR model, using the same number of oscillators as reported in ref 22. This model has the potential advantage of obtaining more physically meaningful parameters, since it takes into account a vibronic progression commonly present in polymer absorption and emission spectra.[33] However, it should be noted that theoretical calculations of absorption spectra[33] commonly obtain an agreement with experimental data that is simply not good enough for device performance modeling. Thus, a compromise between theoretical, semiempirical, and empirical models might be necessary depending on the final purpose of the modeling.

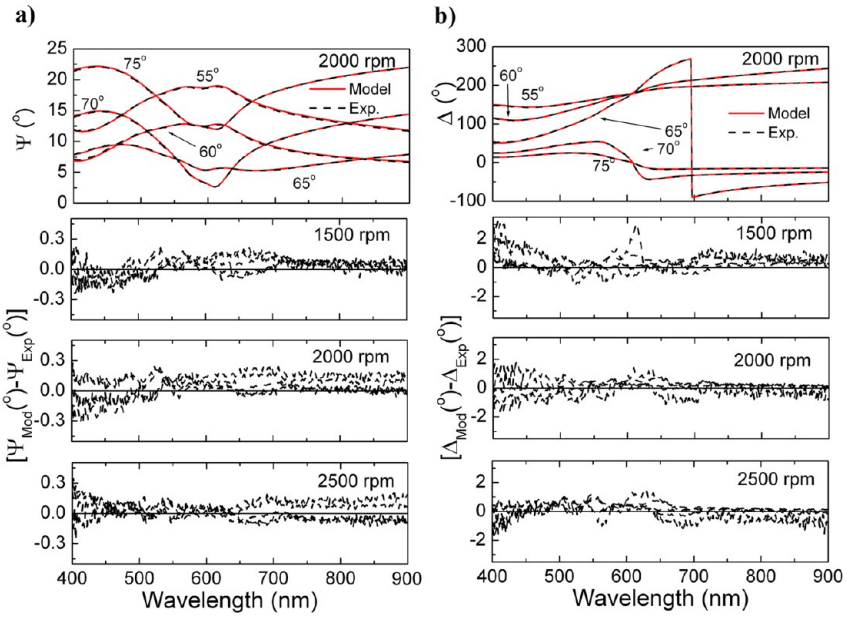

Figure 1. Experimental and calculated (a) Ψ (at 2000 rpm) and residual values (difference between calculated Ψ_{Mod} and experimental Ψ_{Exp} data) and (b) Δ (at 2000 rpm) and residual values (difference between calculated Δ_{Mod} and experimental Δ_{Exp} data) for different spinning speeds at five incident angles for pristine blend film (isotropic GO model, with EMA (pristine P3HT:PCBM blend, 50%)) spin-coated at 1500, 2000, and 2500 rpm. MSE = 3.4.

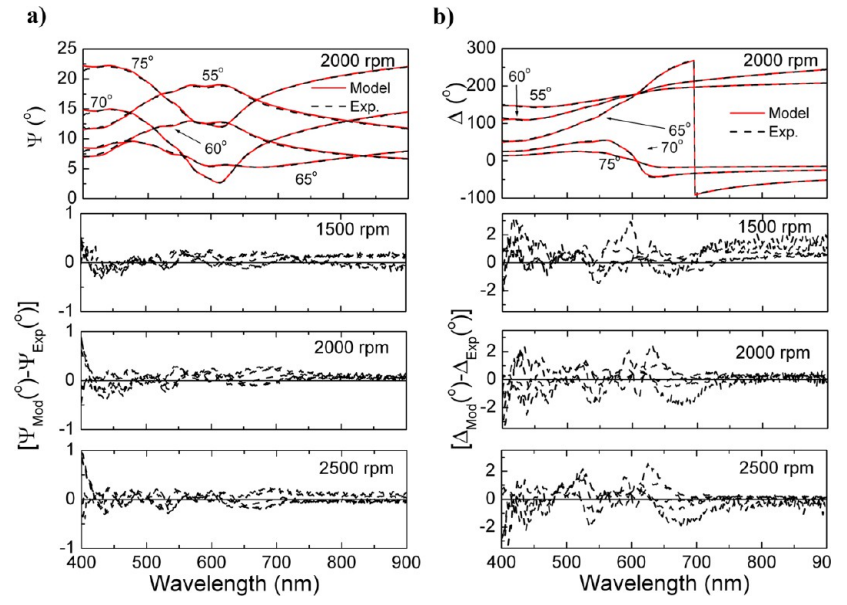

Figure 2. Experimental and calculated (a) Ψ (at 2000 rpm) and residual values (difference between calculated Ψ_{Mod} and experimental Ψ_{Exp} data) and (b) Δ (at 2000 rpm) and residual values (difference between calculated Δ_{Mod} and experimental Δ_{Exp} data) for different spinning speeds at five incident angles for pristine blend film (isotropic HR model, with EMA (pristine P3HT:PCBM blend, 50%)) spin-coated at 1500, 2000, and 2500 rpm. MSE = 4.5.

During the fitting procedure, it was observed that the model parameters corresponding to the extraordinary component of the index of refraction exhibited fitting instability. This issue was addressed using the following procedure. (1) In the initial step, estimates for n and k were obtained by direct inversion using an isotropic model. (2) These values were then fitted using a GO model[8] or HR model,[22] as described previously.[8] (3) The uniaxial optical model was then implemented using the same oscillators from the isotropic model assigned to both ordinary and extraordinary components of the index of refraction; that is, the starting point of the fit is the best achieved isotropic model fitting. As previously mentioned, a large number of parameters resulted in model instability and large parameter uncertainties when all parameters are allowed to vary freely at this stage of the fitting process. Therefore, (4) in the GO model, the oscillator energies of the ordinary and extraordinary components were coupled (thus assuming that the transition energies would be the same, but broadening and oscillator strength could be different), whereas in the HR model, only the amplitudes of HR oscillators, parameters of one Gaussian oscillator, and a pole contribution are allowed to differ between two polarizations (following ref 22.), and a fitting of the "ε_2 only" fitting function was performed, followed by a fit to "ε_1 and ε_2" to obtain a good and physically realistic fit for transmission. (5) In the following step, the standard MSE fitting function was used with the following precaution: whenever any parameter in the extraordinary

components (i.e., F, Γ) exhibited a large uncertainty, it was coupled with its corresponding parameter of the ordinary component and the fitting procedure was repeated. The procedure described resulted in improved fit stability, and in the final step, (6) the coupled parameters were released one at a time until a good fit is obtained with all parameters decoupled and allowed to vary freely except for the thickness of the effective medium approximation (EMA) layer representing the surface roughness, the same as in our previous work.[8]

It should be noted that, regardless of the exact fitting procedure, in some cases, excellent fit is obtained for SE data, whereas transmission data fit could still be far from acceptable depending on the sensitivity of the fitting function used. In our case, the transmission fit can be further improved by increasing the weight of the transmission data that can be set in the "Default" settings of the WVASE software; a similar approach has been reported previously.[22] As expected, however, an excessive increase in the weight of the transmission data could result in decreased quality of Ψ and Δ parameters. After a good fit is obtained in both SE and T data, the final MSE is calculated after reverting the transmission weighting to the default settings. Furthermore, while the proposed approach greatly reduces the occurrence of multiple solutions and/or solutions with unphysical optical functions, it is still necessary to carefully examine the obtained fitting results, in particular, for parallel polarization due to the inherent low sensitivity of SE measurements of thin films on transparent substrates to the extraordinary component of the optical functions.

3. RESULTS AND DISCUSSION

Figures 1−3 show the optical characterization results (SE + T) for P3HT:PCBM with multisample, multiangle-of-incidence analysis for pristine samples using an isotropic GO (Figure 1) and HR (Figure 2) models. The comparison of transmission fitting and the respective *n* and *k* values are shown in Figure 3. The performance of all the models is summarized in Table 1, whereas all the model parameters are given in tables in the Supporting Information.

The corresponding results for annealed blend films using both GO and HR oscillator models are shown in Figures 4−6 for an isotropic model, and Figures 7−9 for an anisotropic model. The fitting parameters are given in the Supporting Information. In this case again, both oscillator models result in similar (poor) performance for the isotropic model, whereas differences for the anisotropic models, which will be discussed in more detail in the following. The representative AFM images of these films are shown in Figure 10.

For pristine films, we can observe that an isotropic model provides a good fit of both SE and T data, where the actual parameters and resulting *n* and *k* obtained exhibit only small differences compared to our previous work.[8] The differences in the optical functions reported here and our previous work for pristine P3HT:PCBM films are likely due to the fact that we used a different blend composition (1:0.8 instead of 1:1), as well as different sources of P3HT (and consequently different molecular weights and polydispersity indexes) and PCBM.[8] This is because we wanted to investigate in detail a material combination that could result in efficiencies close to or exceeding 3%, which would be relevant for modeling P3HT:PCBM solar cells. It should also be noted that P3HT:PCBM blend films with a different P3HT material exhibit different adhesion to the substrate and/or cathode in addition to different photovoltaic performance so that, in some cases, it may be difficult to peel off the electrode after annealing (not the case for the material combination used here). The photovoltaic performance of solar cells is summarized in Table 2, and the corresponding *I*−*V* curves are shown in Figure 11. Clearly, power conversion efficiency exceeding 3%, which is an

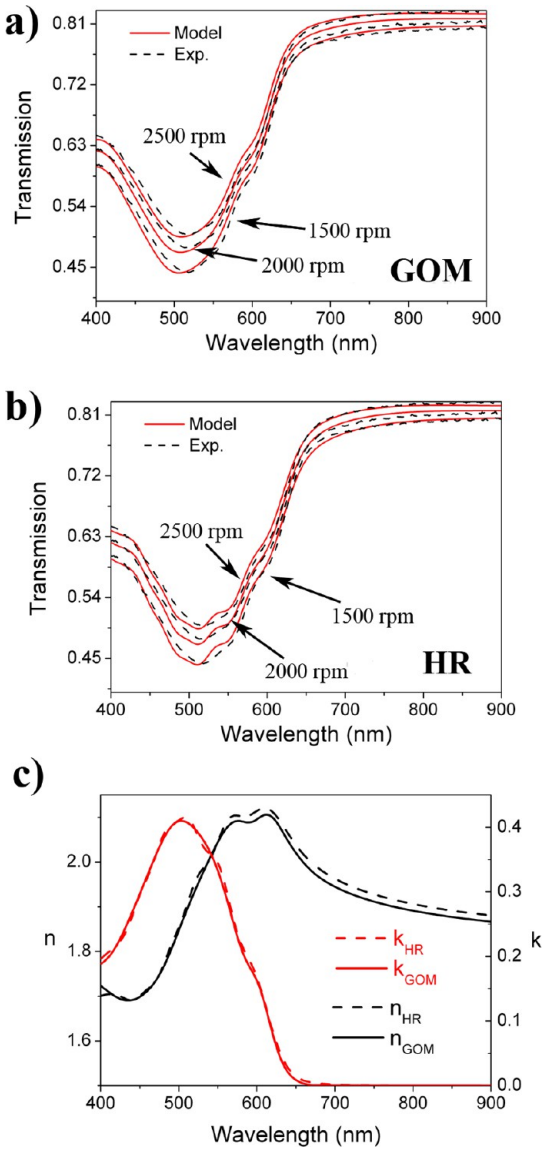

Figure 3. Experimental and calculated transmission data of pristine blend films for (a) GO model and (b) HR model. (c) Obtained *n* and *k* values. MSE = 3.4 for the GO model; MSE = 4.5 for the HR model.

average value for state-of-the-art P3HT:PCBM solar cells,[1] is obtained for solar cells with optimized thicknesses.

After annealing, the roughness of the films increases and the topography changes, as shown in Figure 10. Similar changes in roughness and microphase separation in polymer blend films can also occur as a consequence of solvent annealing or slow drying. Different roughness can also result if a different solvent or different solution concentration is used. Therefore, it is important to independently examine the roughness of the samples (as well as thickness to make a good initial guess) in order to build a realistic sample model for fitting the SE data. In addition, Figures 4−6 show that, while the isotropic model still provides an excellent fit of the SE data, it is no longer possible to simultaneously obtain a good fit to both SE and T data and MSE increases from 3.41 (pristine film, isotropic GO model in Figures 1 and 3) to 22.8 (annealed film, isotropic GO model in Figures 4 and 6). A similar MSE increase can also be observed when using the HR model. These observations make it clear that it is necessary to consider different, more complex models

Table 1. Summary Data of Samples and Optical Models Considered[a]

figure	sample	model	MSE	fit quality
1, 3	pristine P3HT:PCBM	isotropic GO/roughness	3.4	good fit for both SE and T
4, 6	annealed P3HT:PCBM	isotropic GO/roughness, 5 thickness	22.8	good fit for SE, poor fit for T
7, 9	annealed P3HT:PCBM	anisotropic GO/roughness, 5 thickness	18.4	good fit for both SE and T
2, 3	pristine P3HT:PCBM	isotropic HR/roughness	4.5	good fit for both SE and T
5, 6	annealed P3HT:PCBM	isotropic HR/roughness, 5 thickness	23.3	good fit for SE, poor fit for T
8, 9	annealed P3HT:PCBM	anisotropic HR/roughness, 5 thickness	19.6	good fit for SE, poor fit for T
S1	annealed P3HT:PCBM	isotropic GO/roughness, 3 thickness	7.3	good fit for SE, poor fit for T
S2	annealed P3HT:PCBM	anisotropic GO/roughness, 3 thickness	4.6	good fit for both SE and T
S3, S5	annealed P3HT:PCBM	anisotropic GO/no roughness, 5 thickness	17.8	good fit for SE, good fit for T
S4, S5	annealed P3HT:PCBM, GO	anisotropic/no roughness, 5 thickness	17.3	good fit for SE, good fit for T
S6	annealed PCBM, GO	isotropic	5.1	good fit for both SE and T
S7	annealed P3HT, GO	isotropic	6.3	good fit for SE, poor fit for T
S8	annealed P3HT, GO	anisotropic	5.9	good fit for both SE and T
S9	annealed P3HT, HR	isotropic	8.4	good fit for SE, poor fit for T
S10, S11	annealed P3HT, HR	anisotropic	12.3	good fit for SE, poor fit for T
S12	annealed P3HT:PCBM	graded blend Bruggeman (S6−S7) + segregated topmost S6	25.4	good fit for SE, poor fit for T
S13	annealed P3HT:PCBM	graded blend M-G (S6−S7) + segregated topmost S6	29.2	inferior fit for both SE and T
S14	annealed P3HT:PCBM	graded blend linear (S6−S7) + segregated topmost S6	40.7	inferior fit for both SE and T
S15	annealed P3HT:PCBM	graded blend Bruggeman (S6−S8) + segregated topmost S6	43.1	inferior fit for both SE and T
S16	annealed P3HT:PCBM	graded blend M-G (S6−S8) + segregated topmost S6	31.5	good fit for SE, poor fit for T
S17	annealed P3HT:PCBM	graded blend linear (S6−S8) + segregated topmost S6	60.8	inferior fit for both SE and T
S18	annealed P3HT:PCBM	anisotropic HR, roughness, independent parameters	15.4	good fit for both SE and T

[a]Annealing condition in all cases is 150 °C, 15 min. "S" refers to figures in the Supporting Information.

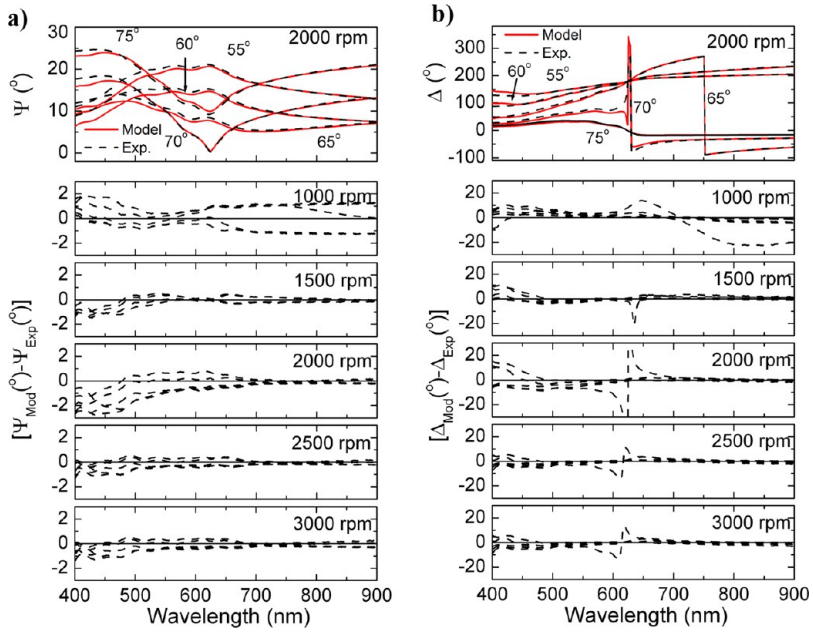

Figure 4. Experimental and calculated (a) Ψ (at 2000 rpm) and residual values (difference between calculated Ψ_{Mod} and experimental Ψ_{Exp} data) and (b) Δ (at 2000 rpm) and residual values (difference between calculated Δ_{Mod} and experimental Δ_{Exp} data) for different spinning speeds at five incident angles for annealed blend film (isotropic GO model, with EMA (annealed P3HT:PCBM blend, 50%)) spin-coated at 1000, 1500, 2000, 2500, and 3000 rpm. MSE = 22.8.

to describe the optical properties of annealed P3HT:PCBM blend films. Such models can include anisotropy, graded film composition, and the presence of segregated layers, as discussed in the Introduction.

Both material segregation and anisotropy can occur as a consequence of annealing, since annealing results in diffusion of blend components as well as crystallization of P3HT domains, resulting in increased order of P3HT chains. In annealed regioregular P3HT films, three peaks could be resolved in the ε''_{xy}, whereas only one peak could be resolved in ε''_{z}.[10] Although anisotropy would likely be less pronounced in blend films compared to pure polymer, it is reasonable to expect that annealing would result in increased order and, therefore, significant anisotropy. Thus, we first considered an anisotropic model fitted following the procedure and precautions outlined in section 2. Figures 7−9 present the anisotropic fit results. Clearly, it is possible to obtain simultaneously a good fit for all film thicknesses for both SE and T data with a final MSE value

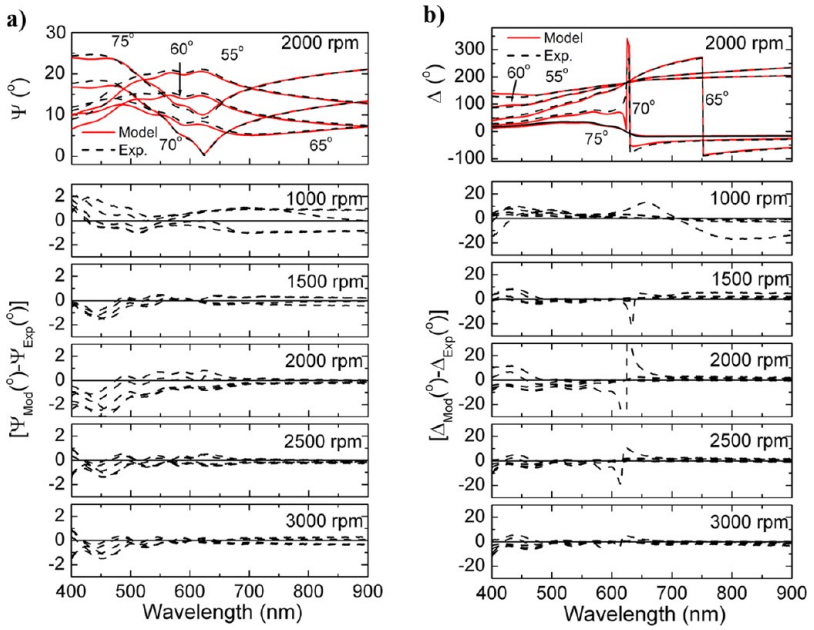

Figure 5. Experimental and calculated (a) Ψ (at 2000 rpm) and residual values (difference between calculated Ψ_{Mod} and experimental Ψ_{Exp} data) and (b) Δ (at 2000 rpm) and residual values (difference between calculated Δ_{Mod} and experimental Δ_{Exp} data) for different spinning speeds at five incident angles for annealed blend film (isotropic HR model, with EMA (annealed P3HT:PCBM blend, 50%)) spin-coated at 1000, 1500, 2000, 2500, and 3000 rpm. MSE = 23.3.

of 18.4 for the GO model and 19.6 for the HR model. Unlike the isotropic case, the difference between the two models is more pronounced, especially in the case of parallel polarization.

The anisotropy of P3HT[10,22] and P3HT:PCBM[11,14,20,22] has been previously reported in the literature. However, no optical functions determination by simultaneous multisample fitting involving both SE and T data has been reported. While for pure P3HT, it has been demonstrated that the data obtained from fitting one thickness could describe P3HT film with different thicknesses[22] (although fit quality should be improved), no such demonstration has been given for anisotropic optical functions of P3HT:PCBM blends.

Anisotropy has been reported in both pristine and annealed P3HT:PCBM blends, with enhanced anisotropy and a significant difference in the shape of ordinary and extraordinary components of the dielectric function (or the complex index of refraction) observed after annealing.[14,20] In another study, a very small anisotropy was observed in P3HT:PCBM blend films before annealing, while significant anisotropy (more pronounced for higher regioregularity) was observed after annealing.[11] In this case, the ordinary and extraordinary spectra of *k* had a similar shape, exhibiting only a difference in the magnitude of the peaks.[11] In the present study, no significant anisotropy is observed before annealing, similar to ref 11; however, we observe anisotropy with significant differences in the shape of the optical functions corresponding to perpendicular and parallel polarizations, similar to refs 14 and 20. Because of the more rigorous fitting procedure (simultaneous fitting of multiple thicknesses for both ellipsometry and transmission data), we believe that we have obtained a more accurate estimate of anisotropy in P3HT:PCBM films compared to previous studies (also, we clearly show that conditions used for our samples are relevant for actual P3HT:PCBM solar cells with an efficiency of ∼3%, which is the average reported efficiency for this material combination[1]).

There are several important issues that should be noted concerning anisotropic model fitting. First, while the obtained result for the perpendicular polarization does not depend on the number of thickness values considered, different values for parallel *n* and *k* are obtained when a 3 thickness or a 5 thickness fitting is considered (see the Supporting Information for the 3 thickness fitting result). We would generally consider fitting results obtained from a higher number of thickness values as more reliable. Since the software allows for simultaneous fitting of 10 data sets (one SE and one T for each thickness), 5 thickness values was the highest number that could be considered. Both solutions (for 3 and 5 thicknesses) were stable; that is, they would not change significantly with continuing attempts to fit the data. Unstable solutions (obtained for different sample models) were not considered reliable. This point serves as another illustration of low sensitivity of SE and T data to the parallel polarization index of refraction in polymer blend films on transparent substrates. One significant issue in selecting the thickness values that would be used for fitting is that samples differing only in spinning speed would be preferable over samples prepared from solutions with different concentrations even though the latter approach could result in a wider range of thickness values. There are two main reasons for this: only a narrow range of thickness values is relevant for high-performance solar cells (see Table 2), and the fact that samples prepared with different solution concentrations may exhibit different microphase separation and, consequently, may no longer have the same *n* and *k* (possible for significant concentration differences). Multisample fitting as an approach to increase the reliability of obtained *n* and *k* is applicable only under the condition that all the films with different thicknesses have the same *n* and *k*.

Second, when fitting without surface roughness is attempted, the fitting result is less stable (i.e., continuing to fit will result in similar MSE values, similar fit quality for SE and T data, similar *n* and *k* for perpendicular polarization, and different solutions

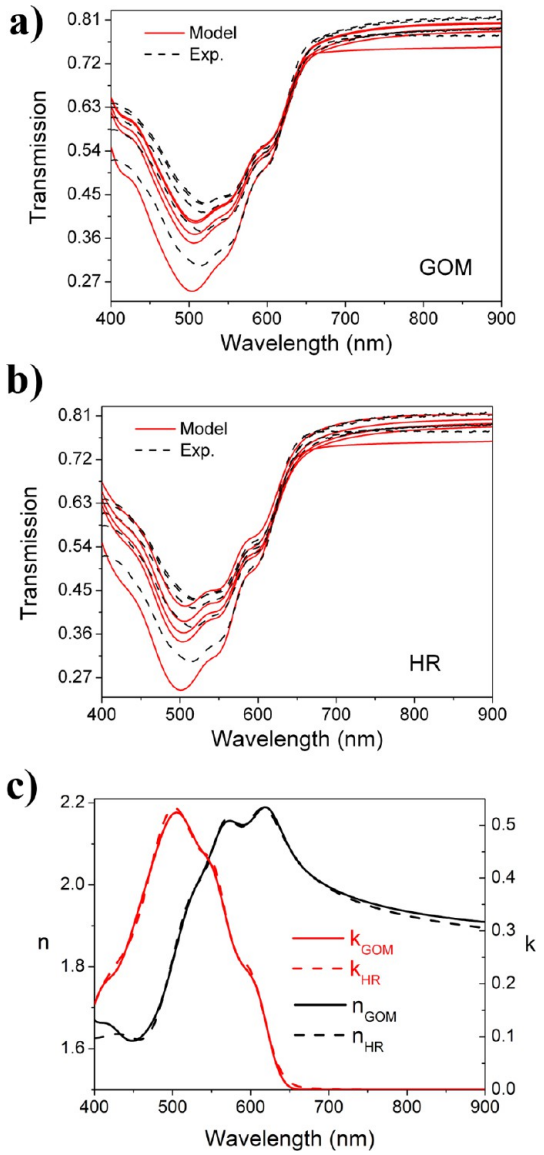

Figure 6. Experimental and calculated transmission data of annealed blend films for isotropic (a) GO and (b) HR models. (c) Obtained *n* and *k* values with EMA. MSE = 22.8 for the GO model; MSE = 23.3 for the HR model.

for *n* and *k* for parallel polarization from one fit attempt to another; see the Supporting Information). This illustrates the importance of using all known sample information (i.e., samples are rough based on AFM measurements) when building a sample model, and again the fact that the data have lower sensitivity to the parallel polarization.

Third, we observe a significant difference in the parallel polarization *n* and *k* for the GO and HR models. In this case as well, both fitting results are stable. In addition to the optical functions difference corresponding to parallel polarization, we can also observe that, for the GO model, a better transmission data fit is obtained compared to the HR model. This would make the GO model more suitable for modeling of the actual solar cells, while the HR model may have some advantage in studying the physical properties of the films where some information about excitonic coupling and the vibronic envelope needs to be extracted from optical data.[22,33] Also, the HR model with coupled parameters has an advantage of being more stable and leading to fewer multiple solutions due to reduced parameter correlations (fewer free parameters, oscillators not totally independent). In the GO model, interpreting the physical value of the obtained parameters is not as straightforward, despite the fact that no unnecessary transitions are considered. In terms of the difference in the optical functions obtained, it should be noted that while the GO model has fewer oscillators compared to the HR model, it has more fitting parameters, which allows it to achieve a better fit (it should be noted that no superfluous transitions, i.e., those that cannot be identified from optical spectra, have been used). In particular, broadenings and energies of the HR oscillators are assumed to be the same, while amplitudes are allowed to vary for the anisotropic sample model.[22] Fit quality could be improved if the parameters in the HR model are allowed to vary (see the Supporting Information). However, in this case, the advantages of fewer model parameters and improved avoiding of getting stuck in local minima due to HR oscillators not being entirely independent are lost. Allowing all parameters to vary can often lead to unstable solutions and unphysical parameter values or parameters stuck at the boundaries (broadenings for oscillators for parallel polarizations, or high values of *S* parameter). In that case, unstable values of broadening can be coupled and more stable solutions in that case can be obtained. Also, one significant difference that we can observe is that *k* for parallel polarization in the HR model commonly goes to very low values at the short wavelength end of the fitting range, λ = 400 nm. Similar behavior can be observed in previously published work using this model.[22] Since P3HT does absorb in the violet and UV spectral range, it is possible that this model does not fully take into account some of the higher-lying transitions. Thus, considering that a better fit is obtained for transmission spectra (important for estimating absorption and consequently external quantum efficiency of actual devices), the GO model is considered to be more suitable if the intended use of extracted *n* and *k* data is solar cell performance simulations. The HR model with more independent parameters can obtain comparable or better fit quality to the GO model, but at the expense of some instability of fitting results for parallel polarization and increased number of free parameters (and consequently reduced reliability of determined parameter values due to possible multiple solutions).

Although excellent fit is obtained with a simple anisotropic layer with a surface roughness correction, as shown in Figures 7 and 9, we also considered an approach of using graded layers and effective medium approximation to model the blend as a combination of P3HT and PCBM.[15,19,20] For this purpose, an isotropic model was considered for PCBM,[20] whereas both isotropic[15,19] and anisotropic[20] models were considered for P3HT (see the Supporting Information). In the case of pure P3HT, we can also observe differences between the GO and the HR models for the *n* and *k* values corresponding to parallel polarization (even more pronounced than in the case of the blend, and with sharp peaks present for the HR model), as well as the quality of the transmission fitting. Since the use of inferior fit for pure P3HT in fitting the blend data would only result in an even worse fitting quality, we will use the GO model in graded layer models. For surface roughness, a segregated PCBM layer was considered.[15] The results and fitting parameters of different models explored are given in the Supporting Information. Similar to blend films, for pure P3HT, it is necessary to take into account anisotropy in order to

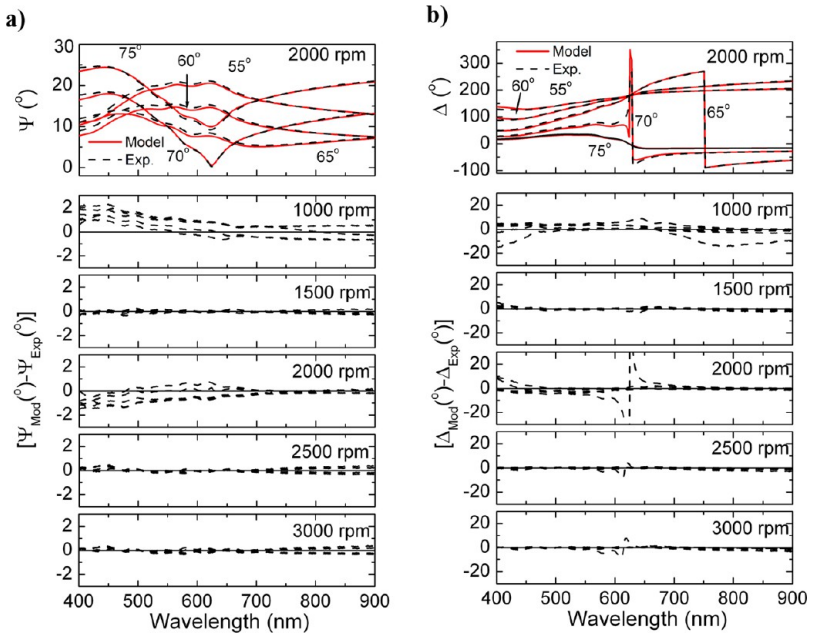

Figure 7. Experimental and calculated (a) Ψ (at 2000 rpm) and residual values (difference between calculated Ψ_{Mod} and experimental Ψ_{Exp} data) and (b) Δ (at 2000 rpm) and residual values (difference between calculated Δ_{Mod} and experimental Δ_{Exp} data) for different spinning speeds at five incident angles for annealed blend film (anisotropic GO model, with EMA (annealed P3HT:PCBM blend, 50%)) spin-coated at 1000, 1500, 2000, 2500, and 3000 rpm. MSE = 18.4.

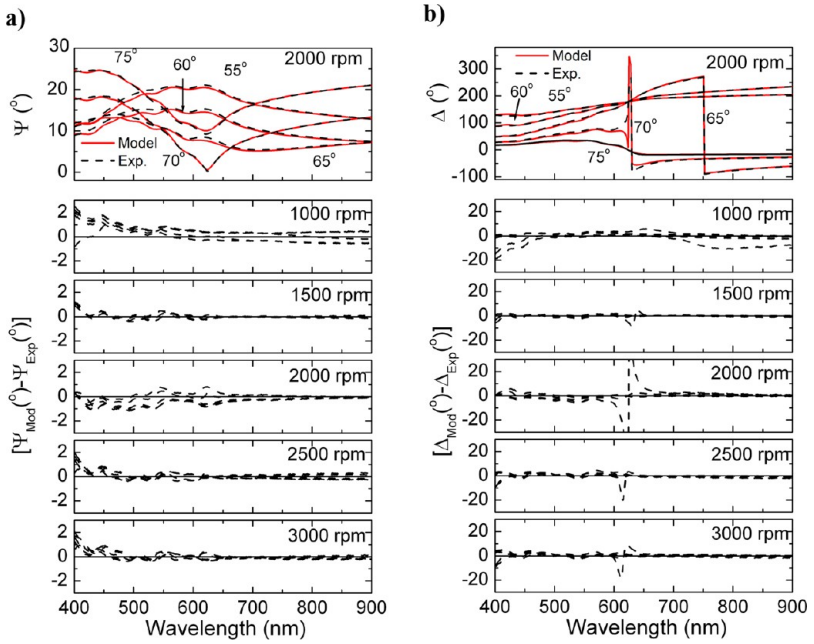

Figure 8. Experimental and calculated (a) Ψ (at 2000 rpm) and residual values (difference between calculated Ψ_{Mod} and experimental Ψ_{Exp} data) and (b) Δ (at 2000 rpm) and residual values (difference between calculated Δ_{Mod} and experimental Δ_{Exp} data) for different spinning speeds at five incident angles for annealed blend film (anisotropic HR model, with EMA (annealed P3HT:PCBM blend, 50%)) spin-coated at 1000, 1500, 2000, 2500, and 3000 rpm. MSE = 19.6.

achieve a good fit of SE and transmission data simultaneously, whereas PCBM could be adequately described with an isotropic model. When graded models using isotropic[15,19] P3HT data or anisotropic[20] P3HT data are used to describe the P3HT:PCBM blend, for all types of EMA (linear, Maxwell–Garnett, and Brugemann)[20] we obtained inferior fit of the data, especially in the case of transmission curves. In addition, it was necessary to couple the PCBM percentage in the samples for SE and transmission measurements. While that is a reasonable assumption (i.e., no big difference in segregation is expected for samples on glass substrates with the only difference in the back surface of the substrate), it is important to note that PCBM content in transmission data fitting tended to go to zero, indicating very poor sensitivity of transmission data to this parameter due to low absorption of PCBM. The inability of graded models to obtain a good simultaneous fit for all sample thickness values and for both SE and transmission data is a clear indication of the unsuitability of the model. One possible

dx.doi.org/10.1021/am4004232 | ACS Appl. Mater. Interfaces 2013, 5, 4247–4259

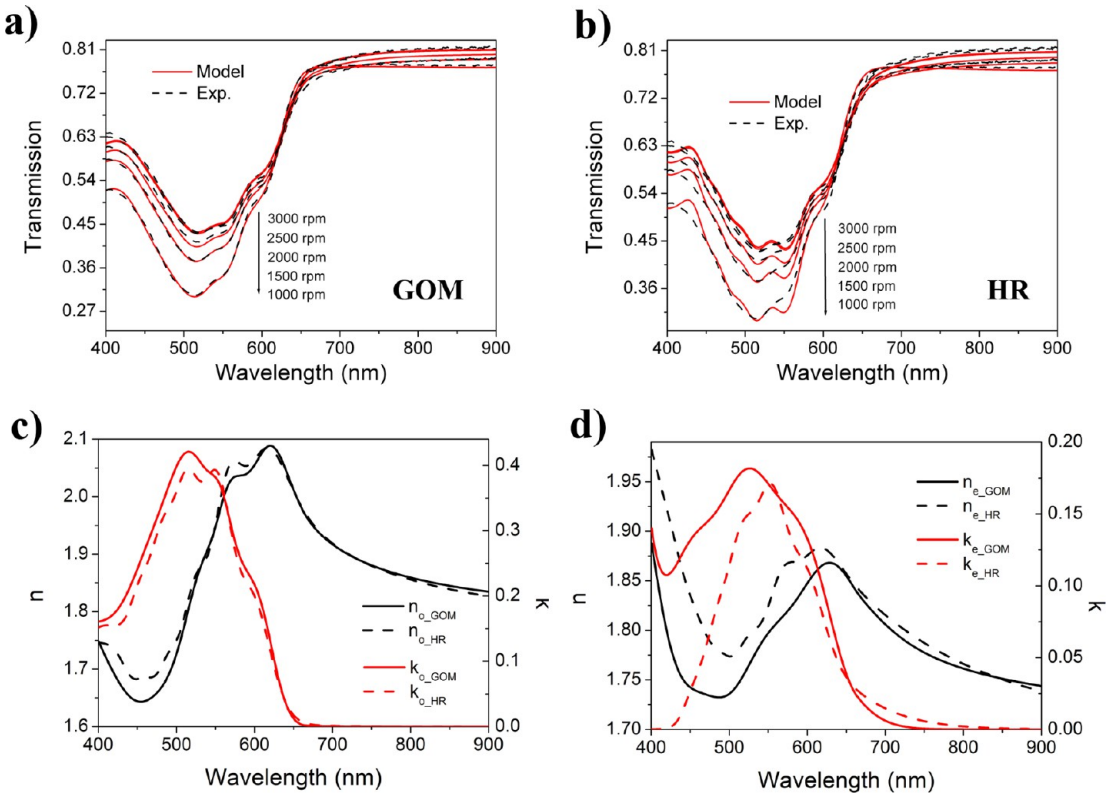

Figure 9. Experimental and calculated transmission data of annealed blend films for anisotropic (a) GO and (b) HR models. (c, d) Obtained *n* and *k* values for perpendicular and parallel polarizations, respectively. MSE = 18.4 for the GO model; MSE = 19.6 for the HR model.

explanation is the fact that organization of P3HT chains is different in pure P3HT films and annealed P3HT:PCBM blend films. Annealed blend films contain domains of crystalline P3HT, but these domains are small since these films actually consist of P3HT domains, PCBM domains, and a mixed phase P3HT:PCBM.[34−36] In fact, about 15−30% of the total PCBM is intermixed with P3HT,[34−36] which would significantly affect the ordering of P3HT chains compared to pure P3HT films. It should be noted that, even in pure P3HT films, it cannot be expected that all polymer chains would be perfectly ordered, and ordering would be further reduced upon incorporation of PCBM. Thus, a simple two-phase EMA model using the optical functions of pure P3HT and pure PCBM would not be able to adequately describe an actual blend layer consisting of P3HT crystals, PCBM crystals, and an amorphous phase of intermixed P3HT and PCBM.[36] The inadequacy of the common EMA-based graded model to describe such a complex structure is also illustrated from the fact that a better fit is obtained using isotropic P3HT compared to anisotropic P3HT, which is a clear indication of the existence of disordered P3HT chains. An even more complex model has been recently proposed, involving low-order P3HT, high-order P3HT, and PCBM, with high-order P3HT described by a uniaxial model.[37] While this is a more realistic model compared to a two-phase EMA, no additional optical data were combined with SE,[37] which lowers the reliability of the obtained fit. Furthermore, the samples for ellipsometry were not annealed and were prepared on Si substrates, different from samples for solar cells that were prepared on ITO/PEDOT:PSS and annealed after the deposition of the Al electrode (which resulted in the best obtained power conversion efficiency of 2.3%).[37] Therefore, even if the complex model used is valid, it may not necessarily apply to high-performance P3HT:PCBM solar cells due to differences in sample preparation for SE measurements and solar cells.

As we already discussed before, the chosen model should be the simplest model that makes physically reasonable assumptions and results in a good fit. In situations where the actual structure of the film may be unknown (for example, preferential segregation of PCBM has been reported to occur at different interfaces by different groups,[38,39] which would require completely different optical models), it cannot be expected that SE measurements would be sufficient to determine whether such segregation indeed occurs, especially in situations where inclusions of such more complicated models result in no significant improvements in the fit quality and increased model parameter uncertainties. More importantly, it is essential to perform a simultaneous fit of samples with different thicknesses, and to consider additional optical measurements (transmission or reflectance) to determine a unique solution that can successfully describe the optical properties of the material. This is particularly important for models including anisotropy, since parameters describing extraordinary components become less stable if transmission is not included (significantly different *n* and *k* obtained in multiple fitting attempts, all with similar MSE), or if fewer thickness values are included, or if roughness is not included. For graded models, including or excluding transmission does not affect the stability of the fit, but calculated transmission data typically exhibit worse agreement with the experiment compared to ellipsometry data if an inadequate model is used (at least for thin polymer films on transparent substrates). In some cases of inappropriate sample models, inferior transmission fit frequently occurs together with estimated film

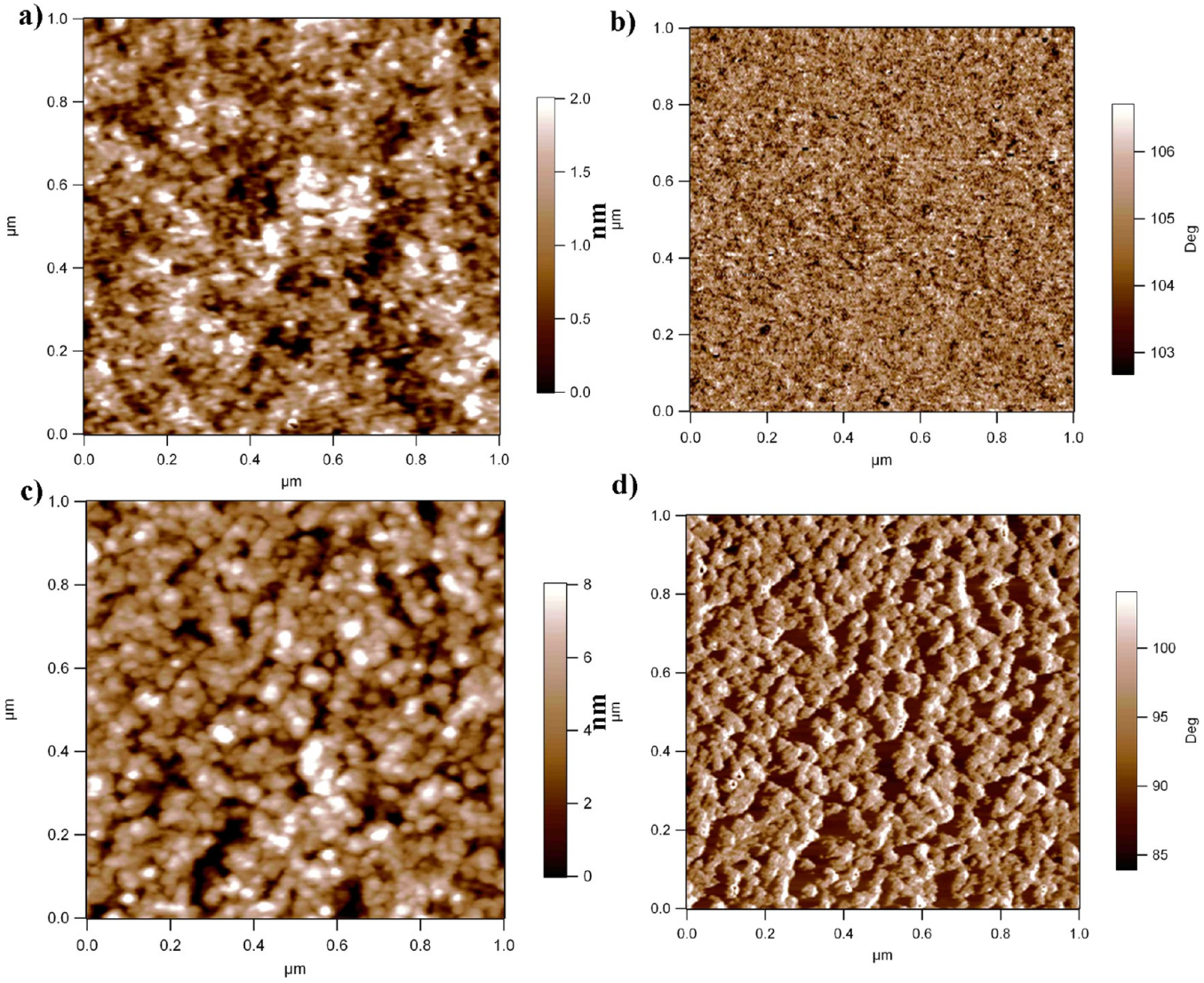

Figure 10. Topography (left) and phase (right) AFM images for (a, b) not annealed P3HT:PCBM (2000 rpm) and (c, d) annealed P3HT:PCBM (2000 rpm).

Table 2. Photovoltaic Performance Parameters (Average of Six Devices) of P3HT:PCBM Solar Cells with Different Spinning Speeds of Blend Solution

	V_{oc} (V)	J_{sc} (mA/cm^2)	fill factor	efficiency (%)
1000 rpm	0.549 ± 0.004	7.2 ± 0.4	0.51 ± 0.01	2.0 ± 0.1
1500 rpm	0.58 ± 0.002	8.9 ± 0.1	0.57 ± 0.01	2.9 ± 0.1
2000 rpm	0.600 ± 0.003	8.5 ± 0.1	0.63 ± 0.01	3.2 ± 0.1
2500 rpm	0.59 ± 0.01	8.5 ± 0.2	0.57 ± 0.02	2.8 ± 0.1
3000 rpm	0.58 ± 0.01	6.9 ± 0.2	0.56 ± 0.01	2.3 ± 0.1

thickness values that deviate significantly from the ones determined by other nonoptical methods, such as scanning electron microscopy.

4. CONCLUSIONS

We have investigated the effect of annealing on the optical properties of P3HT:PCBM blend films (under realistic annealing conditions that result in solar cells with an efficiency ∼ 3%). The optical properties were studied using a combination of spectroscopic ellipsometry and transmission measurements with simultaneous fitting of multiple samples to ensure reliability of the extracted optical functions. We found that it was necessary to take into account the anisotropy of annealed blend films to accurately describe their optical properties. We also found that two different oscillator models resulted in similar n and k values for isotropic sample models and for the n and k corresponding to perpendicular polarization for anisotropic sample models, whereas there were differences in parallel polarization optical functions. In general, n and k corresponding to parallel polarization in an anisotropic model were highly sensitive to the model used, the number of thickness values considered for fitting, and the inclusion of surface roughness. A simple anisotropic model with surface roughness correction was superior compared to various graded

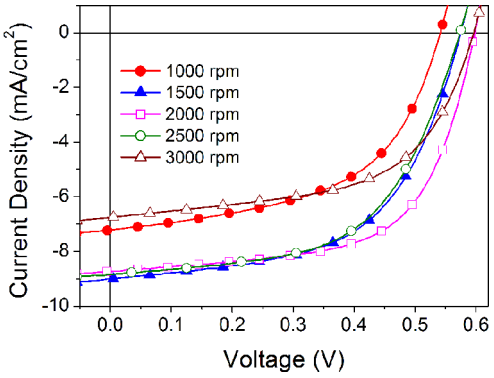

Figure 11. *I*–*V* characteristics of P3HT:PCBM solar cells with different spinning speeds of blend solution.

layer models in simultaneous fitting of SE and transmission data for samples with different thicknesses.

■ ASSOCIATED CONTENT

Ⓢ Supporting Information

Fitting results for the pure PCBM isotropic model, pure P3HT isotropic and anisotropic models (generalized oscillator model and model including Huang–Rhys vibronic envelope), different EMA-based graded models for P3HT:PCBM blend film, anisotropic generalized oscillator model for annealed P3HT:PCBM blend film without surface roughness, and with surface roughness, but for fewer thickness values included in multisample fitting; the anisotropic HR model with uncoupled parameters for annealed P3HT:PCBM blend film; model parameters for all models considered. This material is available free of charge via the Internet at http://pubs.acs.org.

■ AUTHOR INFORMATION

Corresponding Author

*Fax: +852 2559 9152 (A.B.D.), +852 3442-0538 (J.A.Z.). E-mail: dalek@hku.hk (A.B.D.), apjazs@cityu.edu.hk (J.A.Z.).

Notes

The authors declare no competing financial interest.

■ ACKNOWLEDGMENTS

The support of this work by the Strategic Research Theme, University Development Fund, and Small Project Grant (administrated by The University of Hong Kong) is acknowledged. J.A.Z. acknowledges funding from GRF Project 103409 from the Research Grants Council of Hong Kong.

■ REFERENCES

(1) Dang, M. T.; Hirsch, L.; Wantz, G. *Adv. Mater.* **2011**, *23*, 3597–3602.
(2) Yao, Y.; Hou, J.; Xu, Z.; Li, G.; Yang, Y. *Adv. Funct. Mater.* **2008**, *18*, 1783–1789.
(3) Dang, M. T.; Wantz, G.; Bejbouji, H.; Urien; Mathieu, U.; Dautel, O. J.; Vignau, L.; Hirsch, L. *Sol. Energy Mater. Sol. Cells* **2011**, *95*, 3408–3418.
(4) Ma, W.; Kim, J. Y.; Lee, K.; Heeger, A. J. *Macromol. Rapid Commun.* **2007**, *28*, 1776–1780.
(5) Kim, Y.; Cook, S.; Tuladhar, S. M.; Choulis, S. A.; Nelson, J.; Durrant, J. R.; Bradley, D. D. C.; Giles, M.; McCulloch, I.; Ha, C.-S.; Ree, M. *Nat. Mater.* **2006**, *5*, 197–203.
(6) Reyes-Reyes, M.; Kim, K.; Carroll, D. L. *Appl. Phys. Lett.* **2005**, *87*, 083506.
(7) Moulé, A. J.; Meerholz, K. *Adv. Mater.* **2008**, *20*, 240–245.
(8) Ng, A.; Li, C. H.; Fung, M. K.; Djurišić, A. B.; Zapien, J. A.; Chan, W. K.; Cheung, K. Y.; Wong, W.-Y. *J. Phys. Chem. C* **2010**, *114*, 15094–15101.
(9) Campoy-Quiles, M.; Etchegoin, P. G.; Bradley, D. D. C. *Synth. Met.* **2005**, *155*, 279–282.
(10) Gurau, M. C.; Delongchamp, D. M.; Vogel, B. M.; Lin, E. K.; Fischer, D. A.; Sambasivan, S.; Richter, L. J. *Langmuir* **2007**, *23*, 834–842.
(11) Chuang, S. Y.; Chen, H. L.; Lee, W. H.; Huang, Y. C.; Su, W. F.; Jen, W. M.; Chen, C. W. *J. Mater. Chem.* **2009**, *19*, 5554–5560.
(12) Zhokhavets, U.; Erb, T.; Gobsch, G.; Al-Ibrahim, M.; Ambacher, O. *Chem. Phys. Lett.* **2006**, *418*, 347.
(13) Erb, T.; Zhokhavets, U.; Hoppe, H.; Gobsch, G.; Al-Ibrahim, M.; Ambacher, O. *Thin Solid Films* **2006**, *511–512*, 483–485.
(14) Zhokhavets, U.; Erb, T.; Hoppe, H.; Gobsch, G.; Sariciftci, N. S. *Thin Solid Films* **2006**, *496*, 679–682.
(15) Campoy-Quiles, M.; Ferenczi, T.; Agostinelli, T.; Etchegoin, P. G.; Kim, Y.; Anthopoulos, T. D.; Stavrinou, P. N.; Bradley, D. D. C.; Nelson, J. *Nat. Mater.* **2008**, *7*, 158–164.
(16) Koynov, K.; Bahtiar, A.; Ahn, T.; Bubeck, C.; Hörhold, H.-H. *Appl. Phys. Lett.* **2004**, *84*, 3792–3794.
(17) Campoy-Quiles, M.; Schmidt, M.; Nassyrov, D.; Peña, O.; Goñi, A. R.; Alonso, M. I.; Garriga, M. *Thin Solid Films* **2011**, *519*, 2678–2681.
(18) Malgas, G. F.; Motaung, D. E.; Arendse, C. J. *J. Mater. Sci.* **2012**, *47*, 4282–4289.
(19) Karagiannidis, P. G.; Kalfagiannis, N.; Georgiou, D.; Laskarakis, A.; Hastas, N. A.; Pitsalidis, C.; Logothetidis, S. *J. Mater. Chem.* **2012**, *22*, 14624–14632.
(20) Engmann, S.; Turkovic, V.; Gobsch, G.; Hoppe, H. *Adv. Energy Mater.* **2011**, *1*, 684–689.
(21) Wang, T.; Pearson, A. J.; Lidzey, D. G.; Jones, R. A. L. *Adv. Funct. Mater.* **2011**, *21*, 1383–1390.
(22) Morfa, A. J.; Barnes, T. M.; Ferguson, A. J.; Levi, D. H.; Rumbles, G.; Rowlen, K. L.; van de Lagemaat, J. *J. Polym. Sci., Part B: Polym. Phys.* **2011**, *49*, 186–194.
(23) Patterson, L. A. A.; Carlsson, F.; Inganäs, O.; Arwin, H. *Thin Solid Films* **1998**, *313–314*, 356–361.
(24) Hilfiker, J. N.; Singh, N.; Tiwald, T.; Convey, D.; Smith, S. M.; Baker, J. H.; Tompkins, H. G. *Thin Solid Films* **2008**, *516*, 7979–7989.
(25) Ma, W.; Yang, C.; Gong, X.; Lee, K.; Heeger, A. J. *Adv. Funct. Mater.* **2005**, *15*, 1617–1622.
(26) Tompkins, H. G. *A User's Guide to Ellipsometry*; Academic Press Inc.: Boston, MA, 1993.
(27) Fujiwara, H. *Spectroscopic Ellipsometry: Principles and Applications*; John Wiley & Sons: Chichester, England, 2007.
(28) Van der Hofstad, T. G. J.; Di Nuzzo, D.; van den Berg, M.; Janssen, R. A. J.; Meskers, S. C. J. *Adv. Energy Mater.* **2012**, *2*, 1095–1099.
(29) Vandewal, K.; Tvingstedt, K.; Inganäs, O. *Phys. Rev. B* **2012**, *86*, 035212.
(30) Lee, J. Y.; Vandewal, K.; Yost, S. R.; Bahlke, M. E.; Goris, L.; Baldo, M. A.; Manca, J. V.; Van Voohris, T. *J. Am. Chem. Soc.* **2010**, *132*, 11878–11880.
(31) Goris, L.; Haenen, K.; Nesládek, M.; Wagner, P.; Vanderzande, D.; De Schepper, L.; D'Haen, J.; Lutsen, L.; Manca, J. V. *J. Mater. Sci.* **2005**, *40*, 1413–1418.
(32) Österbacka, R.; An, C. P.; Jiang, X. M.; Vardeny, Z. V. *Science* **2000**, *287*, 839–842.
(33) Spano, F. C. *Chem. Phys.* **2006**, *325*, 22–35.2.
(34) Parnell, A. J.; Cadby, A. J.; Mykhaylyk, O. O.; Dunbar, A. D. F.; Hopkinson, P. E.; Donald, A. M.; Jones, R. A. L. *Macromolecules* **2011**, *44*, 6503–6508.
(35) Kiel, J. W.; Eberle, A. P. R.; Mackay, M. E. *Phys. Rev. Lett.* **2010**, *105*, 168701.
(36) Yin, W.; Dadmun, M. *ACS Nano* **2011**, *5*, 4756–4768.
(37) Engmann, S.; Turkovic, V.; Denner, P.; Hoppe, H.; Gobsch, G. *J. Polym. Sci., Part B: Polym. Phys.* **2012**, *50*, 1363–1373.

(38) Orimo, A.; Masuda, K.; Honda, S.; Benten, H.; Ito, S.; Okhita, H.; Tsuji, H. *Appl. Phys. Lett.* **2010**, *96*, 043305.
(39) Kiel, J. W.; Kirby, B. J.; Majkrzak, C. F.; Maranville, B. B.; Mackay, M. E. *Soft Matter* **2010**, *6*, 641−646.